Supporting Information for

Inhibition of CDC42 activity strengthens bone structure after hematopoietic stem cell transplantation.

Theresa Landspersky[1], Merle Stein[2], Mehmet Sacma[3], Johanna Geuder [4], Krischan Braitsch[1], Jennifer Rivière[1], Franziska Hettler[1], Sandra Romero Marquez [1], Baiba Vilne[5], Erik Hameister[1], Daniel Richter [2], Emely Schönhals[1], Jan Tuckermann[2], Mareike Verbeek[1], Peter Herhaus[1], Judith S. Hecker[1], Florian Bassermann[1], Katharina S. Götze[1], Wolfgang Enard[4], Hartmut Geiger[3], Robert A.J. Oostendorp[1]*, Christina Schreck[1]*

[1] Department of Internal Medicine III, Klinikum rechts der Isar, Technische Universität München (TUM), Munich, Germany

[2] Anthropology and Human Genomics, Faculty of Biology, Ludwig-Maximilians University (LMU), Munich, Germany

[3] Institute of Molecular Endocrinology, Ulm University, Ulm Germany

[4] Institute of Molecular Medicine, Ulm University, Ulm, Germany

[5] Laboratory for Bioinformatics, Rīga Stradiņš University, Riga, Lettland

*: joint senior authors and corresponding authors

Christina Schreck, Ph.D.
Technical University of Munich
School of Medicine
Dept. of Internal Medicine III
Ismaningerstrasse 22
81675 München (Germany)
Tel.: +49 89 4140 6318
Fax: +49 89 4140 6057
Email: christina.schreck@tum.de

Robert A.J. Oostendorp, Ph.D.
Technical University of Munich
School of Medicine
Dept. of Internal Medicine III
Ismaningerstrasse 22
81675 München (Germany)
Tel.: +49 89 4140 6056
Fax: +49 89 4140 4826
Email: robert.oostendorp@tum.de

This PDF file includes:

Supporting Information Text

Methods

Mice

In this study, 129S2/SvPasCrl (129), B6.SJL-Ptprca.Pep3b/BoyJ (Ly5.1, CD45.1), and C57BL/6J (B6, CD45.2) mice were obtained from Charles River Labs (Sulzfeld, Germany). 129 were bred with either Ly5.1 (F1: 129Ly5.1) or B6 (F1: 129B6) and the F1 litters were used for the experiments (Supplemental Table S1).

For the transplantation experiments (HSCT group), we utilized 129Ly5.1 mice (3 months old) as donors and 129B6 mice (3 months old) as recipients. Controls were also performed in the reverse manner (HSCT from 129B6 to 129Ly5.1, data not shown). We employed this approach to investigate various facets of interaction between the two mouse strains while concurrently considering the potential influences arising from distinct genetic backgrounds. Our rationale was to gain a comprehensive understanding of the mechanisms underlying the observed changes. We were unable to detect any differences (data not shown), which is why for the analyses, all conducted transplantations were pooled together and normalized.

Age-matched (no transplantation, middle aged, up to 13 months) and young (129Ly5.1, 3 months old) mice were included in the experiments as control groups. To establish their age categories, we employed the concept of "Mouse Age Equivalent," considering the accelerated life cycle of mice relative to humans. A frequently employed conversion formula is: 1 human year is equivalent to 9 mouse days (3 months corresponds to approx. 10 years in humans; 13 months to approx. 45 human years; (2).

All animal experiments were approved by the Government of Upper Bavaria (Vet_02-14-112, Vet_02-15-228, 02-17-124, Vet_03-17-46), and conducted in accordance with ethical guidelines and approved protocols. Mice were housed in specific pathogen–free conditions in the Center for Preclinical Research (TranslaTUM, Munich, Germany) as recommended by the Federation of Laboratory Animal Science Associations.

Murine MSPC isolation and culture

Long bones were flushed (for HSCs) and crushed, followed by digestion as described (for MSPCs) (3). After digestion, flushed or released cells were used for flow cytometry analysis and cell sorting. The remaining bone fragments were plated (0.1% gelatin coating) and the adherent cells were cultured until p3 (80% confluency) in a humidified atmosphere, 5% CO2 and at 37°C in MEM Alpha w/ribonucleic acids, Glutamax, 10% FCS, 1% Pen/Strep, and 0.1% β-Mercaptoethanol. Cell numbers were determined and reseeded ($1 \cdot 10^3$ cells/cm^2) for different cell culture assays at passage 4 (p4), unless stated otherwise.

Human MSPC samples, isolation and culture

Human BM samples were collected with informed consent from healthy individuals. For the healthy samples aged over 60 years, we excluded the presence of clonal hematopoiesis (CHIP) (4). Human BM samples were also obtained from alloHSCT patients with various malignant hematopoietic conditions. All data, both from healthy donors and patients, were normalized and combined for analysis. Use of patient materials were approved by the institutional review board at Technical University of Munich, School of Medicine, Munich, Germany (study TUM 538/16). Characteristics of healthy individuals and patient's treatment regimens used prior to alloHSCT can be found in Supplemental Table S4. Human MSPCs were cultured in low-glucose MEM ALPHA, supplemented with 2 mM L-glutamine, 10 U/L heparin, and 20 U/ml penicillin-streptomycin. Freshly prepared pooled human platelet lysate, at a concentration of 10% (v/v), was added to the cell culture following previously described methods (1, 5).

Fluorescence-activated Cell Sorting (FACS)

Mice were bled monthly by puncturing the facial vein. Peripheral blood was collected in EDTA-coated vials and analyzed using an Animal Blood Cell Counter. Additionally, staining for specific surface markers was performed as described (1, 6). Hematopoietic lineage- SCA1+ KIT+ (LSK) cells and their HSC-enriched CD34- CD48- CD150+ subpopulations (LT-HSCs) were isolated from flushed BM using fluorescently labeled antibodies (Supplemental Table S2). Stromal subpopulations were sorted or analyzed as nonhematopoietic (CD45- TER119-) cells, as described (1, 6). All devices used in this study are listed in Supplemental Table S3, and the gating schemes are shown previously (1).

In vivo transplantation assay

For the initial transplants, $2.5 \bullet 10^5$ whole BM cells were intravenously transplanted into lethally irradiated (8.5Gy) recipient mice, as previously described (1, 6). Peripheral engraftment of donor cells was analyzed every four weeks until ten months post HSCT, when the mice were sacrificed for more detailed analyses.

Treatment with pharmacological compounds

For in vitro assays, MSPCs (passage 4) were cultured with the CDC42/RhoGDI inhibitor CASIN (TOCRIS, #5050, Batch No.2, 5µM) or a vehicle (DMSO) for four hours before starting cell culture assays. In vivo experiments were conducted using CASIN (TOCRIS, #5050, Batch No., 22.4 mg/kg) or the vehicle (PBS and 15% Ethanol) (1). After HSCT on day zero, the compounds were administered via intraperitoneal injection (i.p.) every 24 hours for four consecutive days (5, 6, 7, and 8).

Enumeration of fibroblastoid colonies (CFU-F)

To estimate the frequency of fibroblastoid colony-forming units (CFU-F), MSPCs (p4) were seeded at 300 cells/cm^2. The number of colonies per well was counted 9 to 12 days later.

Micro-CT

Isolated bones were fixed in 4% PFA in PBS for three days and then stored in 70% ethanol. Micro CT was performed using the SkyScan1176 µCT scanner (Supplemental Table S3) at 50Kv, 500mA with a 50µm aluminium filter, 9µm voxel size, and a 1° rotation step. The software packages NRecon, Data Viewer, CTAn, and CTVol (Bruker) were used for analyses and image generation. For tissue mineral density measurements, bones were re-hydrated in PBS for 24h and phantoms of 0.25g and 0.75g CaHA/cm^3 (Bruker) were scanned the same day for calibration.

Human bone mineral density (BMD) measurements

Post-alloHSCT, patients underwent annual BMD measurements for a minimum of five years as per institutional guidelines. BMD was assessed via quantitative computed tomography of the lumbar spine. The QCT PRO Mindways 6.1 software (https://www.qct.com/QCTPro.html) was utilized. It was published by researchers at the University of California for calculating T-scores and Z-scores, which are critical for assessing bone mineral density (BMD) against standardized norms. These scores are derived from the US (UCSF) Normal Database for females and males, which includes BMD data across a wide age range (1–80 years) from healthy US Caucasian or Asian individuals who were ambulatory and had no history of diseases or medication use known to impact bone metabolism like the chronic use of medications such as corticosteroids, thiazide diuretics, or other drugs known to influence bone health. Otherwise, the UCSF database included women who have gone through normal menopause and are taking hormone, calcium, or vitamin D therapy unless they are under 40 years old.

T-Scores and Z-Scores were obtained retrospectively from patient records, with informed consent (ethics vote: 423/17 S).

A Z-score is employed to compare an individual's bone density with the average for their age and gender, a T-score is used to compare bone density with the peak value observed in a healthy young adult. A score higher than or equal to -1 is considered normal. A value between -1 and -2.5 is referred to as Osteopenia, a precursor of Osteoporosis. Values lower than -2.5 are diagnosed as osteoporosis. In healthy young individuals, the Z- and T-scores are typically close to 0, signifying that their bone density aligns with age and gender norms or corresponds to the peak bone density of a healthy young adult.

Senescence assay

MSPCs were plated at a density of $2.5 \cdot 10^3$ cells per cm^2. Nutrient starvation was induced by not changing the media for two weeks and the cells subsequently fixed.

Staining (Figure 2): The fixed cells were stained with the Senescence β-Galactosidase (β-Gal) Staining kit (Cell Signaling). As β-Gal acts on X-Gal, it cleaves the molecule, releasing a blue product. This color change can be visually detected directly in the cultured cells, indicating the presence and activity level of the enzyme. Cells showing a blue staining were counted, and a total cell count was performed for each analyzed sample. The average percentage of stained cells compared to unstained cells was calculated from these evaluations.

FACS (Figure 5): The fixed cells were stained with the CellEvent™ Green Senescence Detection kit (Invitrogen). The kit employs a fluorescein-based probe targeted by β-Gal to identify senescent cells. Upon enzymatic cleavage, the probe emits a fluorescent signal detectable at the wavelength of 490/514 nm, enabling sensitive and rapid fluorescence detection suitable for analysis using FACS.

Immunofluorescence staining (IF, confocal IF)

Cultured MSPCs (p3) were reseeded on Superfrost Plus™ slides (Thermo Fisher Scientific) coated with 0.1% gelatin and cultured overnight in MSPC medium. Cells were fixed with 4% PFA in PBS for five minutes, followed by staining using phalloidin or antibodies (Supplemental Table S2). For counterstaining, SlowFade Gold Antifade Reagent with DAPI (Invitrogen) was used in all staining procedures. Pictures were taken using a Leica DM RBE microscope with AxioVision software (Carl Zeiss) using standardized conditions, including consistent light intensity, exposure, and diaphragm settings. Thirty randomly captured cells per sample were imaged at a 100-fold magnification.

For total protein content assessment, the quantity of pixels per cell was evaluated utilizing ImageJ software (v1.52). For evaluating F-actin fiber formation, each field was analyzed for: 1) the overall cell count; 2) the count of cells displaying elongated F-actin fibers; and 3) the count of cells exhibiting intermediate or no F-actin fiber formation.

For the analysis of damaged DNA foci, clear spots indicating staining with the antibody **γ**H2AX in the cell were counted.

For diameter assessment, relief filters visualized contrasts (Adobe Photoshop, Version 21.1.1). After thresholds were set, cell structures were chosen, and length was determined using ImageJ.

Colocalization was evaluated with ImageJ: single cells were selected, the background removed via the rolling ball algorithm, and thresholds adjusted with the "Moment" autothresholding method. The ImageJ "Colocalization" plugin was then used to identify overlapping pixels of two proteins, with

occupied pixel area measured by the "Analyze particles" function. To discern colocalization bias in nuclear or cytoplasmic proximity, the DAPI signal delimited nuclear areas, and nuclear and cytoplasmic fractions were separately assessed.

Confocal fluorescence Images were captured using a Leica SP8 confocal microscope, which featured a 405 nm excitation laser and a white light laser paired with an acousto-optical beam splitter (AOBS). The confocal setup incorporated three distinct detectors: a single photomultiplier tube (PMT) and two hybrid photodetectors (HyD). For operational control, the microscope was interfaced with the Leica Application Suite X software (ver. 3.5.2.18963). The laser specifications were as described (7). Images were captured using 42 nm pixel intervals, a 102 µs pixel dwell duration, and a double line accumulation, all through a Leica HC PL APO 63x/1.30 NA Glycerol immersion lens. The recorded frame measured 37 × 37 µm, with a scanning rate of 700 Hz. The confocal pinhole was set to 1 A.U. Z-stacks of the confocal images were taken with intervals of 330 nm. Assessment of the different parameters as described above.

Assessment of mitochondrial function

To investigate mitochondrial function, the number, diameter and production of reactive oxygen species (ROS) was analyzed. ROS were detected by cultured MSPCs (p4) for 20 minutes at 37°C with CM-H2DCFDA (5 mM, invitrogen) and facsed with FITC-channel. Staining for the mitochondrial outer membrane receptor TOMM20 or MitoTracker was used to assess the number of mitochondria. For TMRM (mitochondrial membrane potential) measurement, cultured MSPC (P4) were stained with TMRM (250 nM TMRM staining solution, Invitrogen) for 30 minutes at 37°C and facsed with FITC-channel.

Oxygen consumption rate (OCR) and extracellular acidification rate (ECAR) were analyzed on a XF96 Extracellular Flux Analyzer (Supplemental Table S3). For this purpose, $5 \bullet 10^4$ MSPCs/96 well were seeded in a 96-well plate, cultured overnight. The next day, cells were cultured in a medium containing 10 mM glucose for one hour under CO_2 free conditions. Data were recorded under standard conditions and post the introduction of 1 mM oligomycin, 1 mM FCCP (carbonyl cyanide 4-(trifluoromethoxy)phenylhydrazone), and 1 mM Rotenone/antimycin A. The uptake of glucose and the release of lactate were assessed using gas chromatography–mass spectrometry.

Bulk RNA-seq library preparation

Transcriptomes of freshly sorted BM MSPCs were assessed by mcSCRB-seq of 13R mice (n=7), age-matched controls (n=10, 13A), and young control mice (n=7, Y). RNA sequencing was performed using prime-seq, a 3′ tagged RNA-seq protocol based on mcSCRB-seq (8). Briefly, 300 cells per sample were lysed in 50 µL RLT Plus Buffer (Qiagen) supplemented with 1 % β-Mercaptoethanol. Following a Proteinase K (Ambion) digest, nucleic acids were isolated using

SPRI Beads and DNAse digested (Thermo Scientific). cDNA was generated using oligo-dT primers containing sample specific barcodes and unique molecular identifiers (UMIs, Supplemental Figure 2B). After reverse transcription all samples were pooled, the pool was cleaned up using SPRI beads, Exonuclease 1 digested and cDNA was amplified using Kapa HiFi polymerase (Roche). cDNA was quantified using the PicoGreen dsDNA assay kit (Thermo Fisher) and quality control was performed using capillary gel electrophoresis (Bioanalyzer 2100). Sequencing libraries were constructed from 0.8 ng of preamplified cleaned up cDNA using the Nextera XT kit (Illumina) and libraries were size-selected for fragments in the range of 300–800 bp. A full step-by-step protocol including primer sequences is accessible at https://www.protocols.io/view/prime-seq-s9veh66.

The final libraries were paired-end sequenced on an Illumina HiSeq1500 instrument. Sixteen bases were sequenced with the first read to obtain cellular and molecular barcodes and 50 bases were sequenced in the second read into the cDNA fragment.

RNA-seq data processing and analysis

Raw fastq files were processed with the zUMIs pipeline (version 2.4.0f) (9) using STAR 2.6. 1c (10). Reads were mapped to the mouse genome (mm10) and Ensembl gene models (GRCm38) were used for quantification of expression levels. MSPC and HSC samples were filtered separately based on the number of genes and UMIs detected. Genes that had less than ten counts in 50% of the samples were filtered out. Samples were normalized using EdgeR (11) and LIMMA (12) was used to remove the batch effect between the two HSC experiments for clustering and visualization. Limma voom was used for differential gene expression analysis.

Statistics

The variance between the compared groups was similar. Although some of the graphs might suggest normal distribution, it's important to note that biological data rarely conform to the assumptions of a normal distribution. Hence the Mann-Whitney test was applied: this method is used when comparing two independent samples. It's essentially a non-parametric alternative to the independent t-test. Rather than comparing means, the Mann-Whitney test compares the medians of two groups to determine if they are statistically different. As an extension of the Mann-Whitney test, the Kruskal-Wallis test was applied when more than two independent samples need to be compared simultaneously. It serves as a non-parametric alternative to the one-way ANOVA. Instead of comparing means, the Kruskal-Wallis test examines if there's a statistically significant difference in the central tendencies (often medians) of three or more groups.

All statistical analyses were conducted using the Prism software package, and the results are presented as mean ± SD.

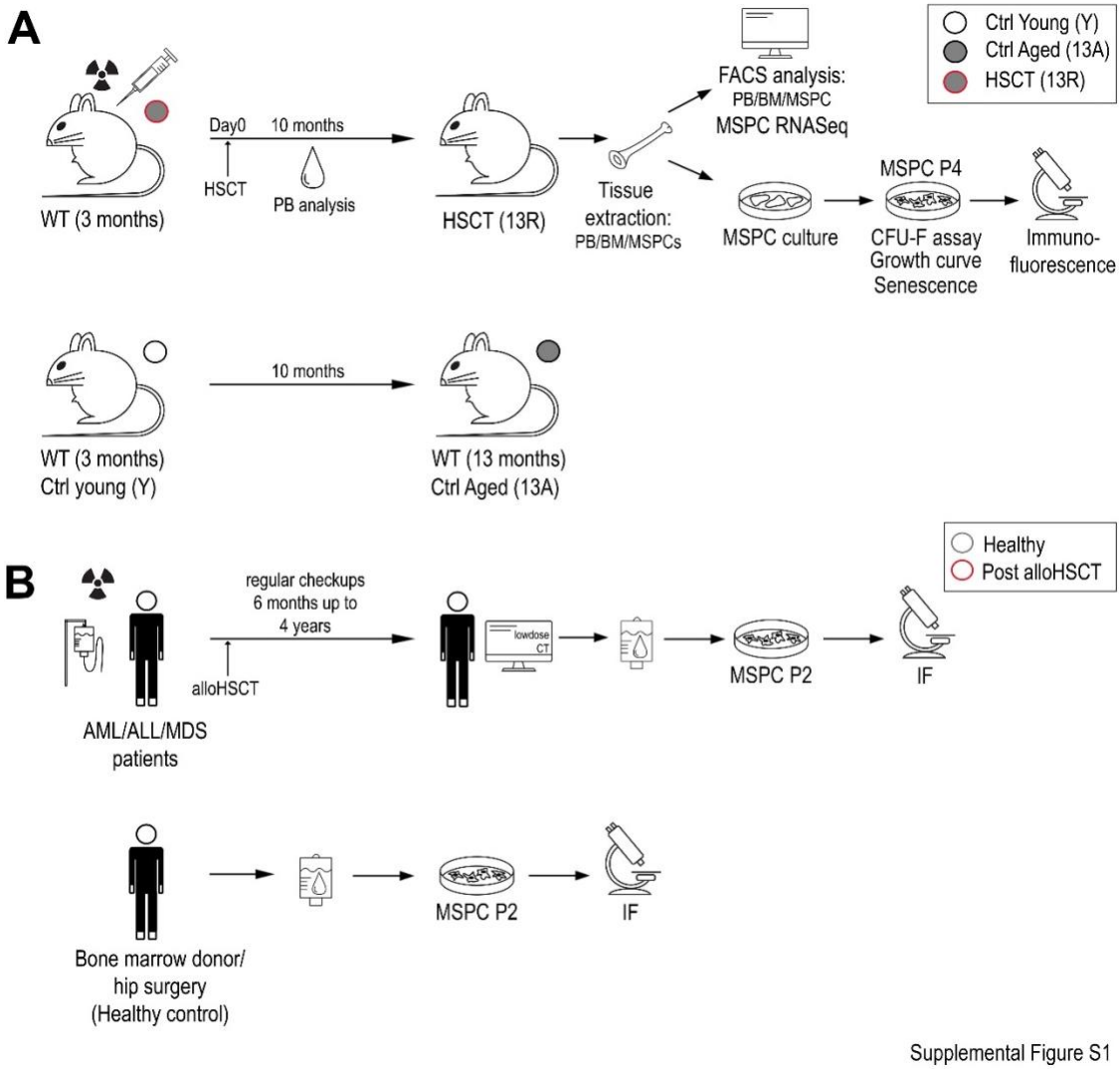

Supplemental Figure S1

Supplemental Figure S1. Experimental design for mouse experiments, human MSC culture and low dose CT analysis (A) Experimental design for hematopoietic stem cell transplantation (HSCT, day 0) into lethally irradiated 3-month-old wildtype mice (timepoint at the end of experiment: 13 months, 13R). Analysis of peripheral blood (PB) within the ten months post HSCT. Tissue extraction in 13-month-old mice (13R): PB, BM and mesenchymal stem and progenitor cells (MSPCs). FACS analysis of isolated PB, BM and MSPCs as well as RNA-seq analysis of sorted MSPCs. MSPC culture out of flushed bones until passage 4 (p4): CFU-F assay, Growth curve and senescence assay. Further staining with Immunofluorescence (IF) assay of P4 MSPCs. Below: Experimental design for control groups: Untreated young control group (Y, 3 months) and untreated age-matched control group (13A). Same analysis as in S1A. (B) Experimental design for human allogeneic hematopoietic stem cell transplantation (alloHSCT) and myeloablation with chemotherapeutic agents and/or irradiation. Patients with Acute Lymphoblastic Leukemia (ALL), Acute Myeloid Leukemia (AML) and Myelodysplastic Syndromes (MDS). Characteristics of patient's treatment regimens used prior to alloHSCT can be found in Supplemental Table S4. Bone marrow (BM) aspirates from regular checkups for human MSC cultivation. IF analysis in P2 human MSCs. Below: Human BM samples were collected with informed consent from healthy individuals (derived from the remains of stem cell transplantation bags or isolated from femoral heads following a hip surgery) and human MSPCs were cultured until P2. Characteristics of healthy individuals can be found in Supplemental Table S4.

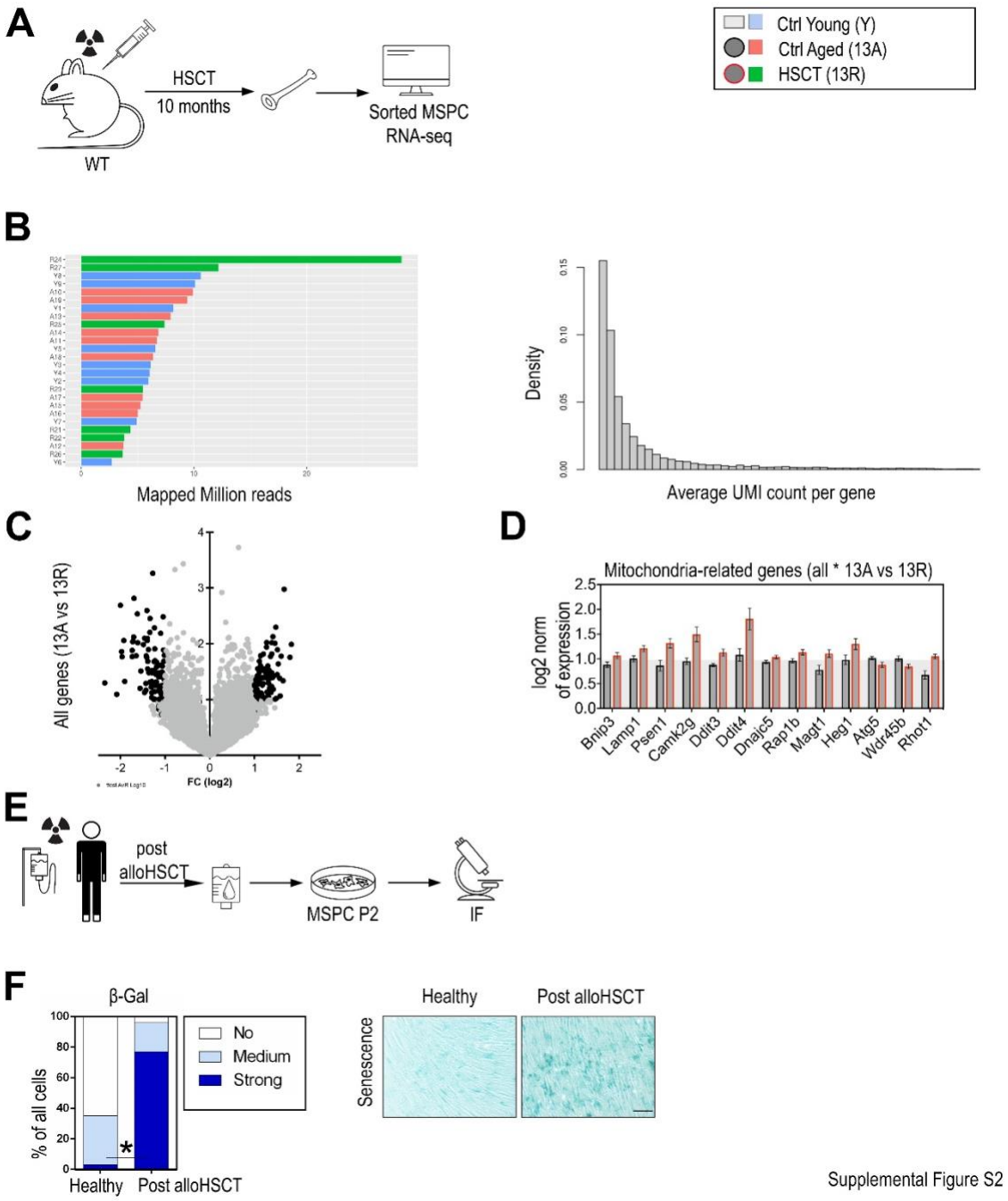

Supplemental Figure S2

Supplemental Figure S2. Hematopoietic stem cell transplantation (HSCT) and permanent changes in MSPCs (A) Experimental design for hematopoietic stem cell transplantation (HSCT) into lethally irradiated 3-month-old wildtype mice (timepoint at the end of experiment: 13 months, 13R). Age-matched control group (13A) without TX. Analysis of the bone marrow (BM) niche in 13-month-old mice (13A and 13R), and young control group (Y, 3 months, data not shown, standard deviation is shown as a grey bar). RNA-seq analysis of sorted MSPCs: Y: n=9, 13A: n=10 and 13R: n=7. (B) Validation of the RNA-seq analysis: Mapped reads for each sample and average of UMI count per gene. (C) Volcano plot showing differential protein expression of all genes between treatment and age-matched control group, with adjusted p-values (FDR) plotted against log2 fold change. 13A: n=10 and 13R: n=7. The dark dots show proteins which meet the FDR threshold for statistical significance (FDR < 0.05) and are considered differentially expressed. (D) Graphs show the expression of mitochondrial related. (E) Experimental design for human HSCT and myeloablation via

chemotherapeutics (n=5) or irradiation (n=2) and analysis from six month up to 24 months post allogeneic HSCT (alloHSCT) in human BM samples. Healthy donor samples as controls (n=6). (F) Average proportion of blue β-Galactosidase (β-Gal) stained compact bone-derived human MSPCs (p2). White bar indicates cells with no detectable staining while light blue refers to partially and dark blue strongly β-Gal stained cells. Representative images of β-Gal stained human MSPCs (P2). The Kruskal-Wallis test was applied here between the three groups examined for each of the three β-Gal staining concentrations (strong, medium, no). The analysis represents one RNA-seq analysis, which was performed with a high amount of samples (Y: n=9, 13A: n=10 and 13R: n=7). Scale bars, 20µm. * p-value < 0.05 (Kruskal-Wallis test: F). Data are represented as mean ± SD.

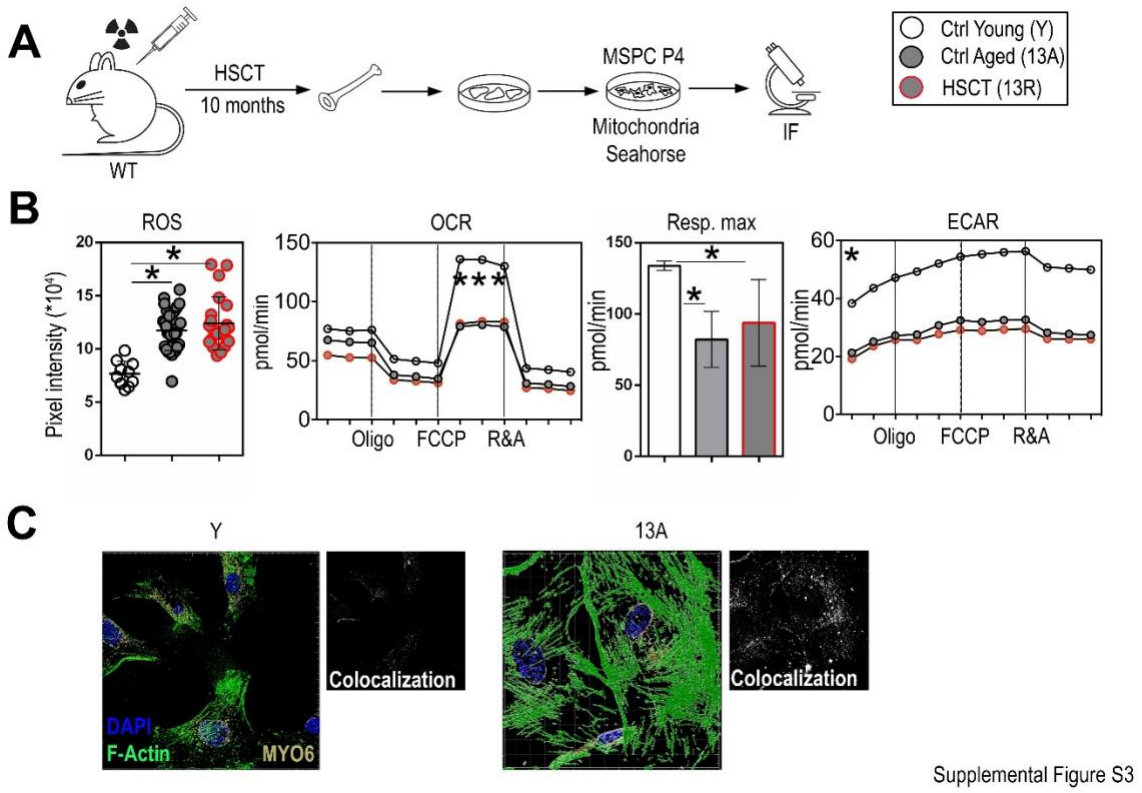

Supplemental Figure S3

Supplemental Figure S3. Mitochondria in MSPCs of HSCT-mice, aged and young controls (A) Experimental design for hematopoietic stem cell transplantation (HSCT) into lethally irradiated 3-month-old wildtype mice (timepoint at the end of experiment: 13 months, 13R). Age-matched control group (13A) without TX. Analysis of cultured mesenchymal stem and progenitor cells (MSPCs) in 13-month-old mice (13A and 13R), and young control group (Y, 3 month). (B) Intensity of reactive oxygen species (ROS) levels in MSPCs. Graph showing pixel intensity measured by ImageJ software (left). Graphs show oxidative phosphorylation (OXPHOS) levels measured by oxygen consumption rates (OCR, left), respiration maximum (middle) and extracellular acidification rate (ECAR, right) in cultured 100% confluent MSPCs (p4). The mean of two independent experiments is shown, four technical replicates per each sample. Y: n=10, 13A: n=6, 13R: n=4; oligo, oligomycin; FCCP, p-trifluoromethoxyphenylhydrazone; R&A, rotenone and antimycin. (C) Representative confocal microscopy images for F-actin (stained in green) and MYO6 (yellow) counterstained with DAPI (blue) with additional visualization of colocalization (white; right) in young (Y) and aged (13A) control MSPCs (P4). (D) Protein content of FABP3 of MSPCs (P4) measured by ImageJ software. The analysis represents two to three independent experiments. Scale bars, 10µm nucleus (DAPI), * p-value < 0.05 (Kruskal-Wallis test: B (ROS); B: nonparametric Mann-Whitney test between all replicates of one group (of each timepoint) compared to all groups (Seahorse assay)). Data are represented as mean ± SD.

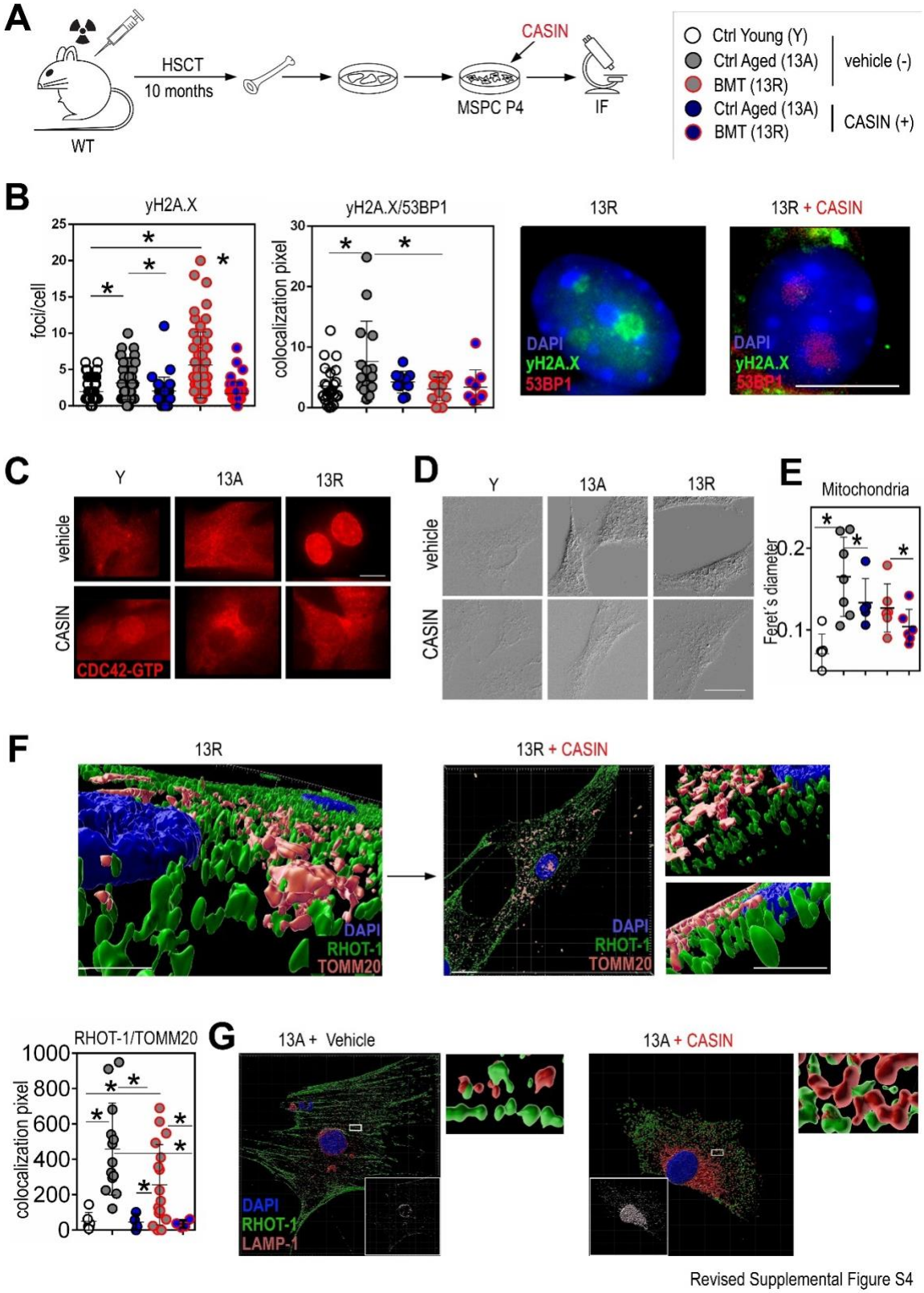

Revised Supplemental Figure S4

Supplemental Figure S4. Pharmacological treatment rescues changes in the MSPCs and mitophagy in MSPCs in vitro (A) Experimental design for hematopoietic stem cell transplantation (HSCT) into lethally irradiated 3-month-old wildtype mice (timepoint at the end of experiment: 13 months, 13R). Age-matched control group (13A) without TX. Analysis of 13 months old mice (13R and 13A) and young control group (Y, 3 months). Mesenchymal stem and progenitor cell (MSPC) culture and CASIN (blue filled symbols) or vehicle (DMSO, grey filled symbols) treatment *in vitro*. (B) Graphs show foci/cell (left) and colocalization pixel of yH2A.X and 53BP1 in the nucleus of cultured MSPCs (p4; middle). Representative Immunofluorescence images of yH2A.X (green) and 53BP1 (red) in compact bone-derived MSPCs (p4; right) counterstained with DAPI. (C) Representative immunofluorescent (IF) microscopy images in cultured MSPCs stained for CDC42-GTP (red) and (D) IF images of mitochondria (TOMM20) in MSPCs illustrated as relief images (Adobe Photoshop: v21.1.1/filter relief) and (E) diameter of mitochondria designated as Feret's diameter measured by ImageJ software. (F) Representative confocal microscopy images stained for Rhot-1 (green) and TOMM20 (red) counterstained with DAPI (blue) of 13R MSPC (P4) with and without CASIN treatment. Image section of mitochondria embedded in RHOT-1 structure. Below: Colocalization pixel of RHOT-1 and TOMM20 measured with ImageJ software. (G) Representative confocal microscopy images for RHOT-1 (stained in green) and LAMP-1 (red) in MSPCs of 13A mice (P4) with and without CASIN treatment. Colocalization is shown in white. The analysis represents two to three independent experiments. Scale bars, 10µm nucleus. * p-value < 0.05 (Kruskal-Wallis test: B, E, F, G). Data are represented as mean ± SD.

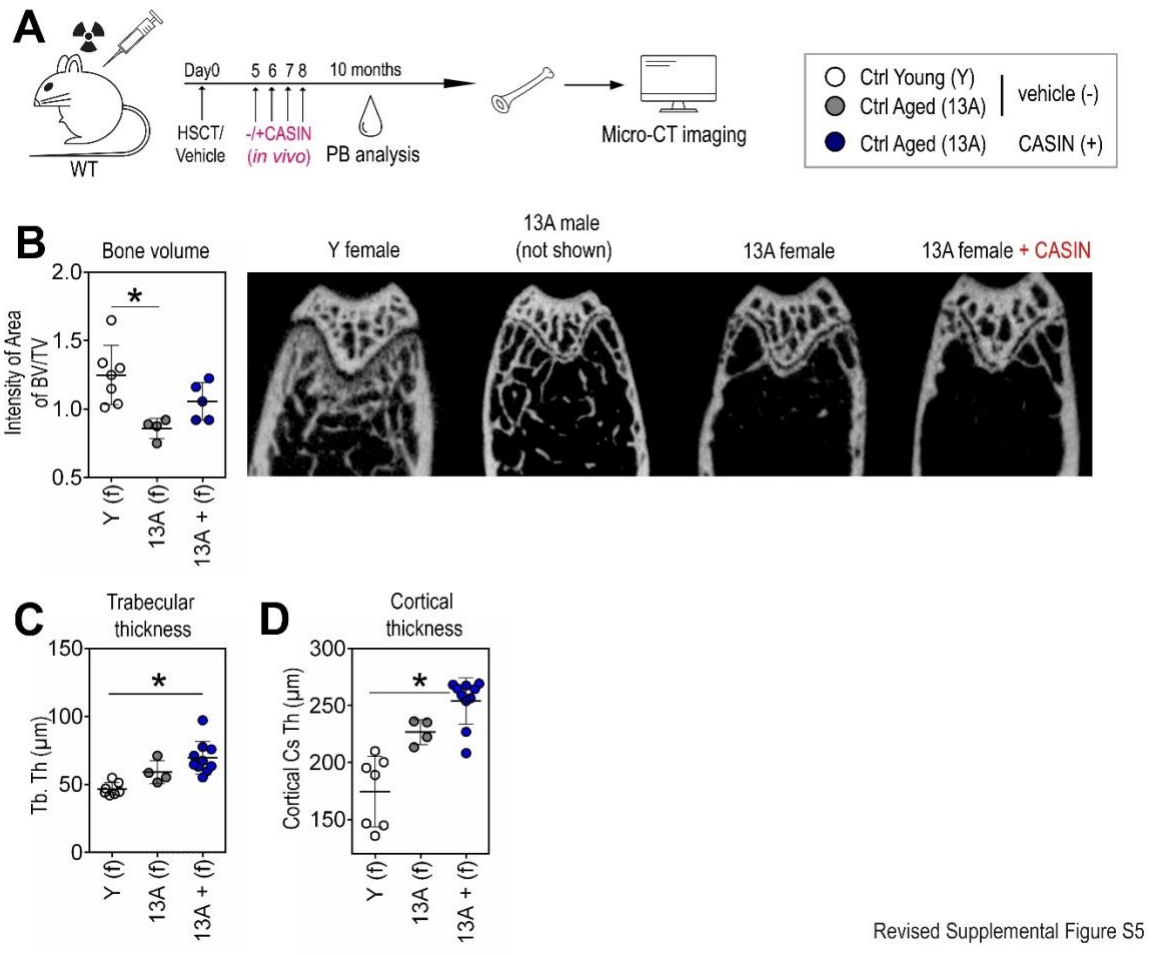

Supplemental Figure S5. Pharmacological treatment accompanying transplantation process modifies bone biology in aged female mice (A) Experimental design for hematopoietic stem cell transplantation (HSCT) into lethally irradiated 3-month-old wildtype mice (timepoint at the end of experiment: 13 months, 13R; not shown). Age-matched control group (13A) without TX. *In vivo* injection of CASIN (intraperitoneal, blue filled symbols) at day 5,6,7, and 8 post HSCT/without TX (13R: not shown; 13A + CASIN). Vector injection (PBS and 15% ethanol, grey filled symbols) at the same time points (13A – CASIN). Analysis of Micro-CT imaging of 13 months old mice (13A) and young control group (Y, 3 months, no HSCT; no CASIN and/or vector treatment). Here the data are just shown for female mice. (B) Micro-CT image of one dissected long bone (femur) per mouse (all males). Percentage of bone volume (BV) in dependence to tissue volume (TV, graph left) measured with Image J software and representative µCT images of Y (females), 13A (males) 13A-/+ CASIN (females) (right). (C) Trabecular thickness analyzed with µCT imaging with representative µCT image of trabecular structures in mouse femur. (D) Cortical thickness analyzed with µCT imaging. The analysis represents two to three independent experiments. The µCT imaging was performed once. * p-value < 0.05 (Kruskal-Wallis test: B, C, D). Data are represented as mean ± SD.

Supplemental Table 1

Experimental Models: Organisms/Strains		
Mouse: 129S2: 129S2/SvPasCrl	Jackson Labs	MGI: 3587894
Mouse: Ly5.1: B6.SJL-Ptprca.Pep3b/BoyJ: B6 Cd45.1	Jackson Labs	MGI: 2164701
Mouse: C57BL/6J: B6 Cd45.2	Jackson Labs	MGI: 3028467

Supplemental Table 2: Antibodies used in this study

	Name	Clone	Fluorochrome	Manufacturer	PRID	Catalog #
Colour controls for surface molecules staining	CD45 Monoclonal Antibody	30-F5	FITC	ebioscience	AB_465050	11-0451-82
	CD45 Monoclonal Antibody	30-F6	PE	ebioscience	AB_465668	12-0451-82
	CD45 Monoclonal Antibody	30-F7	PE-Cy5.5	ebioscience	AB_469718	35-0451-82
	CD45 Monoclonal Antibody	30-F8	PE-Cy7	ebioscience	AB_2734986	25-0451-82
	CD45 Monoclonal Antibody	30-F9	APC	ebioscience	AB_469392	17-0451-82
	CD45 Monoclonal Antibody	30-F10	APC-Cy7	ebioscience	AB_1548781	47-0451-82
	CD45 Monoclonal Antibody	30-F11	PB	ebioscience	AB_10373710	MCD4528
Mature staining	CD3e Monoclonal Antibody	145-2C11	PE-Cy5.5	Invitrogen, eBioscience	AB_11219266	35-0031-82
	TER-119 Monoclonal Antibody	TER-119	PE	Invitrogen	AB_2539207	MA5-17824
	CD45R (B220) Monoclonal Antibody	RA3-6B2	PE-Cy7	Invitrogen, eBioscience	AB_469627	25-0452-81
	Ly-6G/Ly-6C Monoclonal Antibody	RB6-8C5	PB	Invitrogen	AB_10376182	RM3028
	CD11b Monoclonal Antibody	M1/70	APC-Cy7	Invitrogen	AB_2534404	A15390
Transplantation experiments: Mature staining	CD45.1 Monoclonal Antibody	A20	FITC	Invitrogen, eBioscience	AB_465058	11-0453-82
	CD45.2 Monoclonal Antibody	104	PE	Invitrogen, eBioscience	AB_465678	12-0454-81
	CD45R (B220) Monoclonal Antibody	RA3-6B2	PE-Cy7	Invitrogen, eBioscience	AB_469627	25-0452-81
	CD3e Monoclonal Antibody	145-2C11	PE-Cy5.5	Invitrogen, eBioscience	AB_11219266	35-0031-82
	Ly-6G/Ly-6C Monoclonal Antibody	RB6-8C5	PB	Invitrogen	AB_10376182	RM3028
	CD11b Monoclonal Antibody	M1/70	APC-Cy7	Invitrogen	AB_2534404	A15390
HSC staining	CD48 Monoclonal Antibody	HM48-1	Biotin-labeled	Invitrogen, eBioscience	AB_466470	13-0481-82
	Ly-6A/E (Sca-1) Monoclonal Antibody	D7	PE-Cy7	Invitrogen, eBioscience	AB_469669	25-5981-81
	CD117 (c-Kit) Monoclonal Antibody	2B8	PE	Invitrogen, eBioscience	AB_465813	12-1171-82
	CD34 Monoclonal Antibody	RAM 34	FITC	Invitrogen, eBioscience	AB_465021	11-0341-81
	CD150 Monoclonal Antibody	9D1	APC	Invitrogen, eBioscience	AB_469440	17-1501-63
	Mouse Hematopoietic Lineage Biotin Panel		Biotin-labeled	Thermo Fisher Scientific	AB_476399	88-7774-75
	Streptavidin eFluor™ 450 Conjugate		PB	Invitrogen	AB_10359737	48-4317-82
MSC staining	CD45 Monoclonal Antibody	30-F11	PE-Cy5.5	ebioscience	AB_469718	35-0451-82
	TER-119 Monoclonal Antibody	Ter119	PE-Cy5.5	ebioscience	AB_469738	35-5921-82
	Ly-6A/E (Sca-1) Monoclonal Antibody	D7	PE-Cy7	Invitrogen, eBioscience	AB_469669	25-5981-81
	CD31 (PECAM-1) Monoclonal Antibody	390	APC	Invitrogen, eBioscience	AB_657735	17-0311-82
	CD144 (VE-cadherin) Monoclonal Antibody	eBioBV13	PB	Invitrogen, ebioscience	AB_842767	14-1441-82
	CD51 (Integrin alpha V) Monoclonal Antibody	RMV-7	Biotin-labeled	Invitrogen, eBioscience	AB_466477	13-0512-85
	CD166 (ALCAM) Monoclonal Antibody	eBioAlc48	PE	Invitrogen, eBioscience	AB_823125	12-1661-81
	Streptavidin, APC-Alexa Fluor™ 750		APC-Cy7	Invitrogen	AB_2716627	SA1027

	Name	Antigen	Species	Manufacturer	PRID	Catalog #
IF Primary AB	Anti-phospho-Histone H2A.X	Phospho-Histone H2A.X	Mouse	Sigma-Aldrich	AB_309864	05-636
	53BP1 Antibody	53BP1	Rabbit	Novus Biologicals	AB_920462	NB100-304SS
	LAMP-1 Antikörper	LAMP1	Mouse	Santa Cruz	AB_2134495	sc-19992
	Phalloidin-iFluor 488 Reagent	Phalloidin (conjugated Fluor488)		Abcam		ab176753
	Active Cdc42-GTP	CDC42-GTP	Mouse	NewEast Bioscience	AB_1961759	26905
	Recombinant Anti-TOMM20 antibody	TOMM20 (AlexaFluor555)	Mouse	Abcam		ab221292
	RHOT1 Polyclonal Antibody	Rhot-1	Rabbit	Invitrogen	AB_2718689	PA5-72835
	MYO6 Polyclonal Antibody	Myo-6	Rabbit	Invitrogen		PA5-35054
	CM-H2DCFDA (General Oxidative Stress Indicator)	CM-H2DCFDA (ROS)		Life Technologies		C6827
	MitoTracker™ Red CMXRos	Mitotracker		Life Technologies		M7512
	FABP3 Polyclonal Antibody	FABP3	Rabbit	Bioss		BS-11283R
	Optineurin Polyclonal Antibody	Optineurin	Rabbit	Bioss		BS-13658R
	Name	**Antigen**	**Labeling**	**Manufacturer**	**PRID**	**Catalog #**
IF Secondary AB	Goat anti-Mouse IgG (H+L)	Mouse	Alexa Fluor 488	Invitrogen	AB_2534069	A-11001
	Goat anti-Rabbit IgG (H+L)	Rabbit	Alexa Fluor 488	Invitrogen	AB_143165	A-11008
	Goat anti-Mouse IgG (H+L)	Mouse	Alexa Fluor 594	Invitrogen	AB_2534073	A-11005
	Goat anti-Rabbit IgG (H+L)	Rabbit	Alexa Fluor 594	Invitrogen	AB_2534079	A-11012
Name				**Manufacturer**		**Catalog #**
Kits	Senescence β-Galactosidase Staining kit			Cell Signaling, Frankfurt a.M., Germany		#9860
Kits	CellEvent™ Senescence Green Detection Kit			Invitrogen		#C10850

Supplemental Table 3

Equipment and Software		
Animal Blood Cell Counter; Scil Vet ABC	Scil Animal Care, Viernheim, Germany	https://www.scilvet.de/labordiagnostik-fuer-tieraerzte/haematologie/scil-vet-abc-plus
FlowJo 8.8.6	BD Biosciences	https://www.flowjo.com
SkyScan1176 µCT scanner	Bruker, Billerica, MA, USA	http://www.rjl-microanalytic.de/instrumente/bruker-skyscan-mikrotomographie-mikro-ct-nano-ct/
XF96 Extracellular Flux Analyzer	Seahorse Agilent, Waldbronn, Germany	
ImageJ Software	ImageJ NIH	https://imagej.nih.gov/ij/
Software Version Summit 4.4	Beckman Coulter	https://www.bioz.com/result/summit%20software/product/Beckman%20Coulter
FACS Diva Software v8.0	BD Biosciences	https://www.bdbiosciences.com/en-ca/products/software/instrument-software/bd-facsdiva-software
Imaris Software 9.9.0 Oxford	Oxford Instruments	https://imaris.oxinst.com/products/imaris-for-cell-biologists

Supplemental Table 4

Low dose CT Data	Gender	Age*	Classification	Timepoint 1,2,3,4 yrs post HSCT	Radiation	Chemotherapy	Treatments**	Steroids, 0=no, 1=yes
A	male	36	Pre-B-ALL	1,2,3,4	12 Gy TBI	GMALL Protocol	Vitamin D	1
B	male	56	Pro-B-ALL	1,2,3,5	12 Gy TBI	GMALL Protocol	Vitamin D	1
C	male	32	Pre-B-ALL	1,2,3,6	12 Gy TBI	GMALL Protocol	Vitamin D	1
D	female	45	Pro-B-ALL	1,2,3,7	12 Gy TBI	GMALL Protocol	Vitamin D	1
E	female	57	PMF	1,2,3,8	none	Fludarabin/Treosulfan	Vitamin D, Ca2+	1
F	female	28	Common-B-ALL	1,2,3,9	12 Gy TBI	GMALL Protocol	Vitamin D, Ca2+	1
G	female	27	Common-B-ALL	1	12 Gy TBI	GMALL Protocol, Recurrent therapy	None	1
H	female	31	Pro-B-ALL	1	12 Gy TBI	GMALL Protocol	None	1
I	male	55	Pre-T-ALL	1	12 Gy TBI	GMALL Protocol	Vitamin D	1
J	male	60	ALL, Ph+	1	12 Gy TBI	GMALL Protocol + Imatinib	Vitamin D	1
K	male	28	Pre-B-ALL	1	12 Gy TBI	GMALL Protocol	Vitamin D	1
L	male	63	ALL, Ph+	1	8 Gy TBI	GMALL elderly Protocol	Vitamin D, Ca2+	1
M	male	38	Pro-B-ALL	1	12 Gy TBI	GMALL Protocol	Vitamin D	1
N	male	72	AML	1,2,3,4	none	"7+3" ; "7+3"	Vitamin D, Ca2+	1
O	male	52	AML	1,2,3,4	12 Gy TBI	GMALL Protocol	Bisphosphonate, Vitamin D, Ca2+	1
P	male	55	AML	1,2,3	none	"7+3; FLAMSA-RIC	Vitamin D, Ca2+	1
Q	male	73	MDS/MPN-Overlap	1,2,3,4	none	2x Vidaza; Flu/Treo	Vitamin D, Ca2+	1
R	male	73	sAML from MDS	1,2,3,4	none	Vidaza, Flu/Cy/Mel and post-Tx Cy	Bisphosphonate, Vitamin D, Ca2+	1
S	female	48	ALL Ph+	1,2,3,4	12 Gy TBI	GMALL Protocol	Vitamin D	1
T	male	49	AML	1,2,3,4	none	7+3, HDAC, 1. allo with Bu/Cy, Vidaza, FluCyMel	Vitamin D	1
U	female	66	AML	1,2,3,4	none	7+3, 1x Vidaza	Vitamin D, Ca2+	1
V	male	61	MM, MDS	1,2,3,4	none	Vel/CD, Melphalan, FLAMSA-RIC	Vitamin D, Ca2+	0
W	male	43	vSAA	1,2,3,4	none	Flu/Cy	Vitamin D	1
IF staining	**Gender**	**Age***	**Classification**	**Status at biopsy**	**Radiation**	**Chemotherapy**	**Treatments****	**steroids,0=no, 1=yes**
A	male	57	ALL, Ph+	BM	8 Gy TBI	GMALL Protokoll	Vitamin D	1
B	male	66	sAML from MDS	BM	None	1x Azacitidine, FLAMSA-FluCyMel-Ptcy	Vitamin D	0
C	female	54	AML	BM	None	7+3, Kons I, Flu/Treo, Ven/Aza, TFT,	Vitamin D	1
D	male	49	AML	BM	None	7+3, HAM, Flu/Treo	Vitamin D	0
E	female	43	AML	BM	None	7+3, HAM, HDAC, Bu/Cy	Vitamin D	1
F	female	51	AML	BM	12 Gy TBI	ICE, HAM, FluCy (i.R. from TBI/Flu/Cy)	Vitamin D	1
G	male	68	AML	BM	None	7+3 (2x), Kons I-III, HAM, Flu/Treo	Vitamin D	1
Healthy Ctrls IF	**Gender**	**Age***	**Classification**	**Status at biopsy**	**Radiation**	**Chemotherapy**	**Treatments****	**steroids,0=no, 1=yes**
H-A	male	41	healthy	BM	none	none	n/a	0
H-B	female	49	healthy	BM	none	none	n/a	0
H-C	male	51	healthy	BM	none	none	n/a	0
H-D	male	41	healthy	BM	none	none	n/a	0
H-E	female	<60	healthy	BM	none	none	n/a	0
H-F	male	<60	healthy	BM	none	none	n/a	0

Legend: H, healthy sample; AML, acute myeloid leukemia; ALL, acute lymphoid leukemia; PMF, Primäre Myelofibrose; CR, Complete Remission B, Bcell; T, Tcell; n/a, not applicable; BM, bone marrow; GMALL, German Multicenter Study Group for Adult Acute Lymphoblastic Leukemia

* Age at the time of August 10, 2023

** Patient Treatment: Bone-Strengthening Therapy for Osteoporosis

Supplemental Table 5

Changes depending on age (compared to young mice) and changes secondary to HSCT (compared to age-matched controls) plus effects of CASIN treatement								
Figure	**Parameter**	**Y vs 13R**	**13A vs 13R**	**13A vs 13R+C**	**13R vs 13R + C**	**Age**	**HSCT**	**CASIN**
2B	BM cell number	lower	none				X	
2C	% MSPC	none	lower				X	
2C	% OBC	none	higher				X	
2D	CFU-F	lower	lower			X	X	
2E	γH2AX	higher	higher				X	
2F	Senescence	higher	higher				X	
3C	RNAseq		257 DEGs				X	
3E	CDC42-GTP	higher	higher				X	
3F	F-actin fibers	lower	lower			X	X	
3H (human)	CDC42-GTP		higher				X	
3I (human)	F-actin fibers		lower				X	
4C	RHOT-1/TOMM20	higher	none			X		
4D	MYO6/TOMM20	higher	higher			X	X	
4E	MYO6/F-Actin	none	lower				X	
4F	OPTN	lower	lower			X	X	
5B	CFU-F	lower	lower		higher			X
5C	Senescence	higher			lower		X	
5D	CDC42-GTP	higher	higher		lower		X	X
5E	F-Actin	lower	lower	higher	higher		X	X
5H	Mitophagolysosom	lower		higher	higher			
6B	BM cell number	lower			higher			X
6B	%MSPC	none	lower		none			
6B	%OBC	none	higher		lower			X
6C	ROS	higher	higher		lower	X		X
6D	TMRM	lower	lower		higher			X
6E	BV/TV	lower	lower	none	higher	X	X	X
6F	Tb.Th	higher	none	higher			X	X
6G	Co.Th	higher	none	higher			X	X
S2F (human)	Senescence		higher				X	
S3B	ROS	higher	higher			X	X	
S3B	Resp. Max	lower	none			X		
S3C	F-actin/MYO6							
S4B	γH2AX	higher			lower		X	X
S4B	γH2AX/53BP1		lower			X		
S4E	Mitochondria size	none	none	lower			X	X
S4F	RHOT-1/TOMM20	higher	lower	lower		X	X	X

SI References

Sample References:

1. Landspersky T, Sacma M, Riviere J, Hecker JS, Hettler F, Hameister E, et al. Autophagy in mesenchymal progenitors protects mice against bone marrow failure after severe intermittent stress. Blood. 2022;139(5):690-703.
2. Dutta S, and Sengupta P. Men and mice: Relating their ages. Life Sci. 2016;152:244-8.
3. Zhu H, Guo ZK, Jiang XX, Li H, Wang XY, Yao HY, et al. A protocol for isolation and culture of mesenchymal stem cells from mouse compact bone. Nat Protoc. 2010;5(3):550-60.
4. Hecker JS, Hartmann L, Riviere J, Buck MC, van der Garde M, Rothenberg-Thurley M, et al. CHIP and hips: clonal hematopoiesis is common in patients undergoing hip arthroplasty and is associated with autoimmune disease. Blood. 2021;138(18):1727-32.
5. Weickert MT, Hecker JS, Buck MC, Schreck C, Riviere J, Schiemann M, et al. Bone marrow stromal cells from MDS and AML patients show increased adipogenic potential with reduced Delta-like-1 expression. Sci Rep. 2021;11(1):5944.
6. Schreck C, Istvanffy R, Ziegenhain C, Sippenauer T, Ruf F, Henkel L, et al. Niche WNT5A regulates the actin cytoskeleton during regeneration of hematopoietic stem cells. J Exp Med. 2017;214(1):165-81.
7. Hettler F, Schreck C, Marquez SR, Engleitner T, Vilne B, Landspersky T, et al. Osteoprogenitor SFRP1 prevents exhaustion of hematopoietic stem cells via PP2A-PR72/130-mediated regulation of p300. Haematologica. 2023;108(2):490-501.
8. Bagnoli JW, Ziegenhain C, Janjic A, Wange LE, Vieth B, Parekh S, et al. Sensitive and powerful single-cell RNA sequencing using mcSCRB-seq. Nat Commun. 2018;9(1):2937.
9. Parekh S, Ziegenhain C, Vieth B, Enard W, and Hellmann I. zUMIs - A fast and flexible pipeline to process RNA sequencing data with UMIs. Gigascience. 2018;7(6).
10. Dobin A, Davis CA, Schlesinger F, Drenkow J, Zaleski C, Jha S, et al. STAR: ultrafast universal RNA-seq aligner. Bioinformatics. 2013;29(1):15-21.
11. Robinson MD, McCarthy DJ, and Smyth GK. edgeR: a Bioconductor package for differential expression analysis of digital gene expression data. Bioinformatics. 2010;26(1):139-40.
12. Law CW, Chen Y, Shi W, and Smyth GK. voom: Precision weights unlock linear model analysis tools for RNA-seq read counts. Genome Biol. 2014;15(2):R29.